Physica A 202 (1994) 196–223
North-Holland

SDI: 0378-4371(93)E0331-8

PHYSICA A

Dissecting shrimps: results for some one-dimensional physical models

Jason A.C. Gallas

Laboratory for Plasma Research, University of Maryland, College Park, MD 20742-3511, USA
and Höchstleistungsrechenzentrum, Forschungszentrum Jülich, D-52425 Jülich, Germany
and Laboratório de Óptica Quântica, Universidade Federal de Santa Catarina, 88040-900 Florianópolis, Santa Catarina, Brazil

Received 15 June 1993
Revised manuscript received 16 July 1993

This paper describes how certain shrimp-like clusters of stability organize themselves in the parameter space of dynamical systems. Clusters are composed of an infinite affine-similar repetition of a basic elementary cell containing two primary noble points, a head and a tail, defining an axis of approximate symmetry. Knowledge of the axis and the skewness of the k-periodic *main* cell of a $k \times 2^n$ cluster is enough to define the orientation of the whole cluster in space. Peculiarly simple directions along which shrimp-like clusters align are formed by the locus of doubly degenerate *saddle* zero multipliers corresponding to the main shrimp head. In addition, we report a family of models having the boundaries of *all* isoperiodic domains of stability totally degenerate and describe different aspects of their mathematical arrangement and some of their consequences for example, that shrimps are diffeomorphic copies of shrimps.

1. Introduction

A considerable effort has been done so far to understand and classify properties associated with generic bifurcations that appear in mathematical models of natural phenomena. Regarding this topic there is already a relatively large number of results collected in several books, for example, in refs. [1–10]. One interesting development is the observation of Feigenbaum [11] that some behaviors scaling with a geometric rate for quadratic maps are *universal* properties of other dynamical systems and can be calculated with renormalization techniques. This observation has motivated numerous investigations of bifurcation properties of dynamical systems, most notably of maps and differential equations. The original work of Feigenbaum considered families of

unimodal discrete maps of the interval and, perhaps as a consequence, this is the family of systems that since then has by far received the greatest attention. However, during the last ten years or so there has also been work devoted to understand bifurcations of *bimodal* maps. A sample of papers arranged more or less chronologically by topic and discussing specifically the parameter space of bimodal maps are works concerning quartic maps [12], the Hénon map [8,13,14], some circle maps [15–17] and two normal forms of cubic maps [17–19]. Research on these dynamical systems was started more or less simultaneously in the early 80s.

A valuable tool to investigate the structure of the parameter space of dynamical systems is the topological concept of *kneading invariants* [20]. Simply put, by studying the relative ordering of points as they appear in certain periodic sequences passing through critical points of the equations of motion of the system, the so-called superstable orbits, one obtains the locus of superstable parameters, i.e. a continuous curve in parameter space defined by all those and only those parameters corresponding to orbits found (in the space of variables) to go through extrema of the map. The network of parameters corresponding to such superstable orbits was the basic ingredient of the classification schemes discussed in several of the aforementioned works. Thanks to these studies, many important facts are known today about the structure of the parameter space, for example, one knows about the existence of a *skeleton* [15] with *bones* [17]. The mathematical determination and characterization of the whole set of parameters corresponding to superstable orbits involves considering all possible orbits passing through the critical points of a model map of interest. Loosely speaking, the locus of superstable orbits correspond to "centers of stability" of isoperiodic regions. However, apart from knowing the locations of centers of stability, a precious information frequently needed for applications in physics is the precise extent of each individual k-periodic region around such centers. One of the main points of the present paper is to discuss from a totally algebraic point of view how the problem of delimiting the full extent of regions of periodicity may be solved and to implement it on a number of representative cases. Such algebraic approach contributes effectively to abbreviate the stability analysis of physical systems. As shown below in section 6, it also allows one to obtain a number of interesting results which do not seem easy to obtain by other means. Thus, such approach might be of interest as a complement to the topologic approach frequently used nowadays.

The basic motivation of this paper is the wish to understand several regularities recently found [14,19,21] to be present in isoperiodic diagrams of 1D and 2D families of polynomial dynamical systems. By numerically investigating parameter regions corresponding to *stable* periodic orbits for all

periods up to 128, it was possible to obtain a fairly broad view of the way in which bifurcation cascades organize themselves in discrete-time dynamical systems when high-periods are also taken into account. The parameter space contains a number of interesting regularities, for example, it contains many shrimp-like structures, i.e. many complex nestings of isoperiodic shells following $k \times 2^n$ doubling cascades from a *main* k-periodic central body. Such structures were found to appear aligned along very specific simple directions. The main k-periodic region of some of the first few low-period shrimps was already known from earlier studies, for example, from refs. [8,12,13,15–18]. Some of these references may also contain other doubling shells. But the fact that domains of stability appear affine-like aligned along simple directions over extended parameter ranges appears to have been first described in ref. [14].

This paper argues that isoperiodic shrimps result from a countable doubly-infinite affine repetition of a basic elementary cell characterized by ten noble points where specific degeneracies in the dynamics occur. Two *primary* noble points in the cell are their *head* and their *tail*. (A quick look at fig. 7 below might be useful at this point.) A line through these points defines an axis of approximate symmetry for every cell and tells roughly how the cell appears oriented in space. All in all, the fundamental message is that the α direction of ref. [14] (Hénon map) and ref. [19] (two cubic maps) is in fact the *head locus* of the *main* head of every shrimp cluster. Since the equations of motion constrain unambiguously the orientation of the stability domains around the axis, knowledge of the orientation of the axis along with the proper "skewness" of the cell is essentially equivalent to the knowledge of the orientation of the full cluster. The infinite structure-parallel-to-structure sequence [14] of isoperiodic shrimps results from an infinite sequence of affine transformations of a "basic shrimp" in the parameter space which, in their turn, are themselves composed via affine repetitions of a "mother cell". As the periodicity increases, iterative processes going on in the space of variables produce in the parameter space infinite progressions of a two-cycle operation: *distort* and *translate*. Thus, the regular structures reported in refs. [14,19,21] are seen to arise from a doubly-infinite continued repetition of just two relatively elementary operations on a mother cell, or atom. All clusters may be diffeomorphically mapped to a basic cluster which is itself composed of an infinite number of cells obtained diffeomorphically from the mother cell.

We start in the next section, section 2, by recalling a concept that will be our fundamental tool for dissecting the parameter space, the century-old concept of *multipliers*. As an important warm-up, in section 3 we evaluate multipliers for the familiar quadratic map $x_{t+1} = a - x_t^2$. More than a trivial exercise, this example will prepare the ground for discussing the parameter space of physical systems depending on several parameters. In fact, this example is the basic key

for understanding situations involving more parameters. In section 4 we calculate multipliers for one of the two families of cubic maps for which detailed color isoperiodic diagrams have been recently presented [19] and dissect cubic shrimps. Section 5 presents a few interesting dynamical systems resulting from processes involving *compositions* of one or several quadratic maps. In particular, we present a highly symmetric *canonical stability structure* in parameter space. This structure is shown to have degenerate borders and to delimit all domains of stability for isoperiodic motions of families of dynamical systems, e.g. eqs. (5.2) and (5.3) below, having different dimension and following different routes to chaos. In other words, the cartographic subdivision of the parameter space for these quite different dynamical systems contains borders which are *exactly degenerate*, the distinction between each degenerate "lot" in both charts being the periodicity, which depends on the equations of motion. Section 6 dissects the period-1 mother cell from which all others are obtained, shows where the ten noble points of degeneracy occur in this cell and presents explicitly one example of affine transformation for "tunneling" between shrimps of period-1 and shrimps of period $3 \rightarrow 9 \rightarrow \cdots$, etc. In addition, section 6 argues that the period-1 mother cell can be heuristically expected to be the canonical one for a wide class of physical systems. Finally, section 7 summarizes our main conclusions, some of its consequences, and advances a preliminary view of the dynamics of triplets (x, a, b), the "algebra of critical points," as imposed by the equations of motion. The corresponding discussion for multidimensional systems is slightly more involved and will be presented in a separate paper.

2. Definitions and tools for one-dimensional dissections

Whether simple or generalized, isoperiodic structures that we generate in the parameter space correspond always to islands of stability. The basic tool needed to delimit the boundaries of such islands is the concept of *multiplier*. This useful concept may be conveniently borrowed, for example, from the historical works of Fatou [22] and Julia [23] where it was used to analyse the dynamics of rational functions in the complex plane. Multipliers, however, were already used much earlier by Fuchs, by Floquet and by Poincaré among several others.

All variables and parameters considered here are assumed to be real quantities. We study one-dimensional discrete-time dynamical systems written in the usual way as

$$x_{t+1} = f(x_t, a, b) , \quad t = 0, 1, 2, \ldots , \tag{2.1}$$

and, for simplicity, assumed to only depend on two parameters: a and b. All definitions remain valid, however, for any number of parameters. Maintaining parameters fixed, we refer to a sequence of iterates $x_0, x_1, x_2, \ldots$ of eq. (2.1) as an "orbit" or equivalently, "trajectory". Orbits are said to be *periodic* if after eventually a transient regime, they repeat. They are *k-periodic* or *k-cycles* if k is the smallest number of 'clock-units' t between repetitions of the sequence. An arbitrary point x_t in the sequence $\{x_t\}$ is reached by *composing* inductively t times the function f with itself: $f_t \equiv f \circ f_{t-1} = f \circ f \circ f_{t-2}$, etc. The function $f_t(x, a, b)$ so obtained gives then a generic point x_t in the sequence as a function of the initial point x_0, in other words, it connects the generations x_0 and x_t:

$$x_t = f_t(x_0, a, b) . \tag{2.2}$$

It does not seem necessary to overload the notation by introducing a special symbol to explicitly distinguish function compositions from indices of *consequent* points. Note, however, that while formally eqs. (2.1) and (2.2) might look innocently similar, they are in fact very different. For example, if $f(x, a, b)$ is a cubic polynomial, then $f_t(x, a, b)$ will also be a polynomial but with variable and explosive degree: x^{3^t}, i.e. a polynomial which becomes quickly too long to be written down explicitly as t increases.

Let us consider now a generic k-periodic sequence of points

$$x_0, x_1, x_2, x_3, \ldots, x_k \equiv x_0 , \tag{2.3}$$

assumed obtained by iterating eq. (2.1) after discarding eventual transient behaviors. From eq. (2.2) it is clear that x_0 must be a fixed point of f_k. Let us further consider generic points x_t lying very close to the fixed point x_0 and study how they behave as time evolves. For this purpose we build the sequence of differences

$$x_{t+k} - x_0 \equiv f_k(x_t) - f_k(x_0) = (x_t - x_0) f_k' + \text{h.o.t.} , \tag{2.4}$$

where 'h.o.t.' stands for 'higher order terms' in the series expansion. From this expansion it follows that as time evolves

$$\frac{x_{t+k} - x_0}{x_t - x_0} \to f_k' , \tag{2.5}$$

showing that the derivative f_k' rules simultaneously the stability around x_0 and the way in which the sequence $\{x_t\}$ converges/diverges close to the fixed point, either by flipping or by moving continuously to/from the fixed point. The orbit is therefore characterized by the quantity

$$m_k \equiv m(x_k, a, b) = f_k'(x_0, a, b) = \left.\frac{\mathrm{d}f_k(x, a, b)}{\mathrm{d}x}\right|_{x=x_0}, \tag{2.6}$$

which is called the *multiplier* of the orbit in eq. (2.3). By explicitly evaluating the derivative, eq. (2.6) can be conveniently written in the form

$$m \equiv m(x_k, a, b) = f'(x_{k-1})\, f'(x_{k-2})\, f'(x_{k-3}) \ldots f'(x_0)\,, \tag{2.7}$$

which then shows why m was very properly called 'multiplier' quite a while ago. From eq. (2.7) one recognizes a very important property: m is a "mean-field-like" quantity containing cumulative information sampled along *all points* of the trajectory. We explicitly introduced the point x_k into the definition of m as a useful mnemonic index to help keep track of the particular orbit with which m is associated and of its periodicity. Let $M \equiv |m|$. From eq. (2.5), the k-periodic orbit of eq. (2.3) is therefore seen to be *attracting* if $M < 1$, *repelling* if $M > 1$ and *indifferent* if $M = 1$. *Superstable* orbits are those for which $M = 0$. In parameter space, boundaries of k-periodic *cells of stability* are obtained by sweeping a and b and recording those values for which $m_k = +1$ ("fold" or "tangent" or "saddle-node" bifurcations) and $m_k = -1$ ("flip" or "pitchfork" or "period-doubling" bifurcations). This is done by solving the following sets of equations

$$\begin{cases} x = f_k(x, a, b) \\ m_k = +1\,, \end{cases}, \qquad \begin{cases} x = f_k(x, a, b) \\ m_k = -1\,, \end{cases}, \tag{2.8}$$

where k is the period of the cell. With these definitions we are now equipped to study the stability of sequences of points generated by eq. (2.1). As will become clear from the figures to follow, multipliers are extremely valuable tools to investigate the parameter space. By acting as a powerful "X-ray", they expose and facilitate the study of the intrinsic internal structure of stability cells and of any other more complicated structures living in the parameter space. Multipliers sample all points along trajectories and are therefore very sensitive detectors of changes in the dynamics. Observe that Lyapunov exponents are quite simply related to $\log |m|$.

3. Anatomy of unimodal shrimps: a quadratic example

Before considering two parameters, let us first briefly evaluate multipliers for a familiar and simpler situation having just a single parameter, namely, for the quadratic map

$$x_{t+1} = f(x_t, a) = a - x_t^2 . \tag{3.1}$$

In this case $f'(x_t, a) = -2x_t$ and the multiplier of a k-periodic orbit is then

$$m \equiv m_k = (-2)^k x_0 x_1 x_2 \ldots x_{k-1} , \qquad k = 1, 2, 3, \ldots \tag{3.2}$$

From this equation one immediately sees that for the quadratic map, zero multipliers may only occur for those particular orbits containing the point $x = 0$, the *only* possible point where the derivative of the map is zero, a rather atypical situation. Generic physical models are more likely to involve derivatives containing several zeros occurring in many parameter-dependent locations.

Fig. 1 shows the familiar bifurcation diagram for eq. (3.1), together with a plot of the first few m_k. From this figure one recognizes that altogether the multiplier is a piecewise continuous function of the parameter a. Discontinuities exist at relatively few isolated points where *bifurcations* occur, with m changing abruptly from $-1 \rightarrow +1$ (for a increasing) or equivalently, from $+1 \rightarrow -1$ (a decreasing). This shows the *multivaluedness* of multipliers corresponding to *nonhyperbolic* parameters, i.e. those parameters for which $|m_k| = 1$. This multivaluedness is responsible for much of the mathematical difficulty associated with nonhyperbolic periodic orbits. But it is simultaneously responsible for the rich physical multistability and fractal structure found for parameters at the tail region of isoperiodic cells where multipliers are multivalued functions over *extended* domains and hysteretic behavior is typical while varying parameters (see discussion below). The use of $M = |m|$ instead of

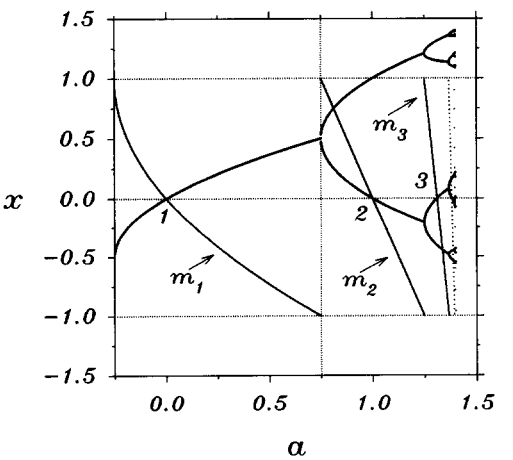

Fig. 1. Multipliers for the quadratic map $x_{t+1} = a - x_t^2$, eq. (3.1).

m hinders the recognition of the multivaluedness at nonhyperbolic parameters. Note that appellations currently used to describe bifurcations assume *implicitly* parameters to vary in specific directions, usually increasing, and completely disregard the important multivaluedness concomitant with the bifurcation process. For example, $m = +1$ is not an exclusive privilege of those parameter values where stability appears to be suddenly created *ex nihilo*. As for any multivalued process, it is important to always keep track of the proper Riemann surfaces involved in discontinuities occurring at bifurcations. Indicated in fig. 1 are also the first three $m_i = 0$ (superstable) orbits which, as mentioned, must always pass through $x = 0$ for the quadratic map. The geometric scaling obeyed by the several bifurcation windows is sensibly reflected in the m curves, and appears as an increase of the spacing between their points as a grows. Note that the slope of the several m_i curves tends very fast to ∞ at the 2^n accumulation point of the cascade. From fig. 1 one sees that, instead of the actual numerical value of m, it might be sometimes convenient and/or enough to characterize regions having identical *parity*, i.e. to characterize a whole sub-region inside a cell using just the sign of m in it. This will be the case in the figures below.

4. Anatomy of bimodal shrimps: a cubic example

From eq. (2.7) one sees that $m = 0$ orbits are those for which the *derivative* of the physical model $f(x, a, b)$ is zero for at least one point along an orbit. While for the quadratic map the derivative had no freedom to be zero at any point other than $x = 0$, the situation may radically change for systems with complicated equations of motion and which will then almost invariably involve more than one parameter. For more complicated maps the derivative may be zero at more than one value of x. Noble points of degeneracy will arise in parameter space when these values of x are simultaneously fixed points of $f_k(x, a, b)$. In this case the question is then to know whether sequences generated by the different x values are the same or not. Since the x are different, most of the times their associated sequences will be different. The only way in which two sequences of iterates corresponding to different fixed points might be equal is if they contain *both fixed points simultaneously*. For high-period sequences, there are in addition *several possible valid permutations* for the occurrence of fixed points along such sequences. In fact, for multiparameter dynamical systems all these degeneracies are exactly the most interesting points to look for. The dynamical behaviour as observed in the space of variables of physical systems is therefore seen to be ruled by the group of all possible permutations of the degenerate fixed points of $f_k(x, a, b)$. This

group is at the origin of the peculiar directions along which shrimps align in parameter space. As the period increases smaller groups of permutations reappear again and again as subgroups of larger groups of permutations. Fortunately, relatively few points inside the unit cell are enough to completely characterize the position and orientation of the full cluster of stability (shrimp) in parameter space. We now address the problem of how to compute them exactly.

Consider the following normal form of a family of cubic maps:

$$x_{t+1} = -x_t(x_t^2 - 3a) - b \,. \tag{4.1}$$

This is one of the two common normal forms of cubic maps [17–19], $x_{t+1} = \pm x_t(x_t^2 - 3a) - b$, to which every other real cubic map can be reduced. Refs. [17,18] present a very nice and detailed discussion of the location of the $m = 0$ centers of stability, i.e. of the locus of superstable orbits in parameter space. Ref. [19] contains many detailed color pictures of the full extent (i.e., for $-1 \leqslant m \leqslant 1$) of each corresponding isoperiodic cell of stability centered on the superstable locus showing precisely how they all are organized. The derivative of eq. (4.1) is $-3(x_t^2 - a)$ and, accordingly, the multiplier of a k-periodic orbits is

$$m \equiv m_k = (-3)^k(x_0^2 - a)(x_1^2 - a)\cdots(x_{k-1}^2 - a) \,, \tag{4.2}$$

implying $m = 0$ whenever $x_j^2 = a$, with the obvious solutions

$$x_j = +\sqrt{a} \quad \text{and} \quad x_j = -\sqrt{a} \,. \tag{4.3}$$

The first three generations of points descending from these two are

$$f_1(\pm\sqrt{a}) = -b \pm 2a\sqrt{a} \,, \tag{4.4}$$

$$f_2(\pm\sqrt{a}) = 12a^3b - 3ab + b^3 - b \pm (6a^2 - 8a^4 - 6ab^2)\sqrt{a} \,, \tag{4.5}$$

$$\begin{aligned} f_3(\pm\sqrt{a}) = {} & -b + b^3 - 3b^5 + 3b^7 - b^9 \\ & + a^5b(108 + 324a - 288a^2 - 2160a^3 + 192a^4 + 4032a^5 - 2304a^7) \\ & + ab^3(9 + 27a - 9a^2 - 432a^3 - 1080a^4 + 720a^5 + 5040a^6 - 5376a^8) \\ & + ab^5(-18 - 27a + 180a^2 + 756a^3 - 2016a^5) + ab^7(9 - 144a^2) \\ & \pm [3a + a^7(-216 + 864a^2 - 1152a^4 + 517a^6) \\ & + a^2b^2(-18 - 108a - 138a^2 + 576a^3 + 2160a^4 - 576a^5 - 6048a^6 + 4608a^8) \end{aligned}$$

$$+ ab^4(18 + 144a + 270a^2 - 480a^3 - 2520a^4 + 4032a^6)$$
$$+ ab^6(-36 - 126a + 672a^3) + 18ab^8]\sqrt{a}\,. \qquad (4.6)$$

Analysis of the genealogy implied by these and similar equations clearly shows that underlying the iterative process there is a generalized algebraic structure with a "projection" along the real axis totally isomorphic to that of the complex numbers, with $\sqrt{a}$ playing the role of $\sqrt{-1}$. In this framework, successive iterations correspond to visiting criteriously chosen *vertices* of a kind of polygonal lattice embedded in the high-dimensional space defined by some generalized numbers, a very peculiar set of numbers containing both real and complex numbers at specific particular limits. The symmetric critical points $+\sqrt{a}$ and $-\sqrt{a}$ are *conjugate* to each other. This structure arises by extending and iterating considerations which show that a quite simple way to obtain the dynamics of any real quadratic $x^2 + \alpha x + \beta = 0$ is by defining $u = -\alpha/2$ and $d = \alpha^2/4 - \beta$ and working with the resolvent $x^2 - 2ux + u^2 - d = 0$. This corresponds to a very convenient optimization of parameters. Solutions for this normal form are readily seen to be now $u \pm \sqrt{d}$, with the sign of d directly "exposing" the nature of vertices, i.e. directly telling whether roots are real or not and whether they may be further reduced to a lower surface. To study the dynamics of iterated quadratic maps one does not need to necessarily extract square roots at every stage. At any rate, for our present purposes it suffices to say that eqs. (4.4)–(4.6) allow one to conveniently choose even or odd combinations of functions (not depending on the signs in eqs. (4.3)) which considerably simplify analytical calculations.

Fig. 2 shows the portion of the parameter space of eq. (4.1) for which the dynamics of most of the parameters is characterized by finite attractors with relatively large basins of attraction. This figure introduces conventions that are also used in several subsequent figures. The basic convention is that regions of similar shadings correspond to regions of similar properties: periodicity in fig. 2a (and similar subsequent "a" figures), and parity of multipliers in fig. 2b (and other similar "b" figures). Integer numbers indicate the periodicity of the main cell (i.e. of the k-periodic cell of every $k \times 2^n$ cluster). Fig. 2a contains explicitly indicated the regions of period 1 and 2 which, as all other regions, have a symmetric counterpart with respect to the $b = 0$ line. There are also two period-3 regions centered along the line $a = 0.364\ldots$, as indicated. In this and similar figures, white shadings are used to represent parameters for which generic initial conditions near $x_0 = 0$ lead to chaotic attractors. The symbols $-\infty$ and $+\infty$ reflect the structure of a Cantor set of initial conditions confined between the two extreme turning points of the cubic "potential": this complex structure may be identified as being a sort of measure giving the "diffusion-time" needed for tunneling beyond the turning points and to start from there

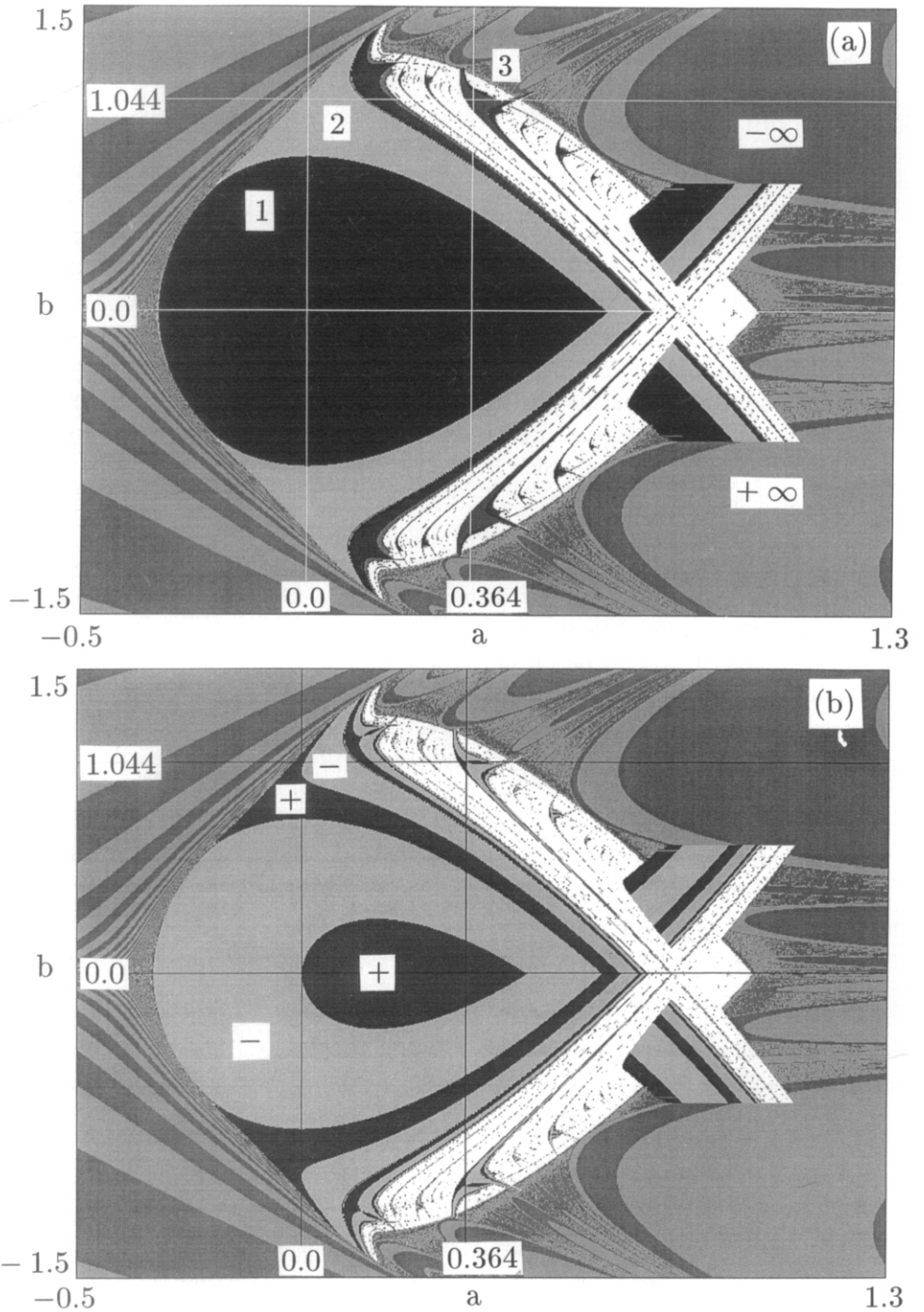

Fig. 2. Basic stability region for the cubic map $x_{t+1} = -x_t(x_t^2 - 3a) - b$, eq. (4.1). Similar shading indicates identical periodicities. White regions correspond to chaos. (a) Isoperiodic domains, numbers indicating periods; (b) parity of multipliers, eq. (4.2). The intersection of the lines at $a \simeq 0.364$ and $b \simeq 1.044$ indicates the location of head of the period-3 shrimp shown further magnified in figs. 3 and 4.

to move towards infinity either by flipping or moving steadily, depending on the sign of the cubic term. Finer details in this region correspond to points lying deeper and deeper in the Cantor set. Fig. 2b presents "m-ray" views of the internal structure of every domain of stability, made possible by using two shadings to represent the parity of the multiplier corresponding to each individual point (a, b). The parity of the first few larger regions is as indicated and also defines the shading convention used. In the (relatively small) regions of multistability the figures present features as obtained for *one* of the possible attractors, usually that with the largest basin of attraction near $x_0 = 0$. All isoperiodic diagrams in this paper involve a 1024×768 grid of equally spaced points in the $a \times b$ plane, respectively, consider periods higher than 128 as chaos and were computed by forward-incrementing a along lines of constant b using some convenient initial value for the orbit (typically $x_0 = 0$). We *followed the orbit* [14a], i.e. used the last obtained x_i as the initial condition to compute the periodicity for every newly incremented value of a. (As opposed to the other simple possibility: to *restart* each orbit repeatedly from one and the same x_0.)

Part of the upper portion of fig. 2 is shown magnified in fig. 3, with fig. 4 showing a much closer view of the period-3 shrimp. This sequence of magnifications allows one to recognize the great regularity of the internal structure of all isoperiodic shrimp clusters. From figs. 2, 3 and 4 one sees that shrimps are composed of a perfectly countable infinite affine repetition of a self-similar basic "cell" or "atom", each one containing two fundamental points: a *head* and a *tail*. A line through them is an axis of approximate symmetry for each individual cell. Internally, every cell is symmetrically divided into four adjacent *quadrants*, characterized by the parity of the multiplier, and centered on the unique *saddle point* which defines the head. Border lines between regions of different parity are loci of $m = 0$ parameters, i.e. parameters corresponding to the superstable orbits studied previously in refs. [15–18], for example. Each cell contains two lines of superstability: one corresponding to orbits passing through the point $x = +\sqrt{a}$, the other to those through $x = -\sqrt{a}$. Figs. 2 and 3 show that the alignment of shrimps previously found in refs. [14,19,21] corresponds to the *heads locus* of the main isoperiodic regions. This head locus should not be confused with the known locus of superstable orbits [15–18]. As seen from the figures, the head locus corresponds to a *discrete sequence of points* in the parameter space. It contrasts with loci of superstable orbits which are continuous curves. Since altogether the cells composing shrimps are structures rigidly attached to each other by the dynamics, from the figures it is clear that to fix the relative orientation of a full shrimp in parameter space one essentially needs to know two fundamental quantities: the relative orientation of the approximate axis of

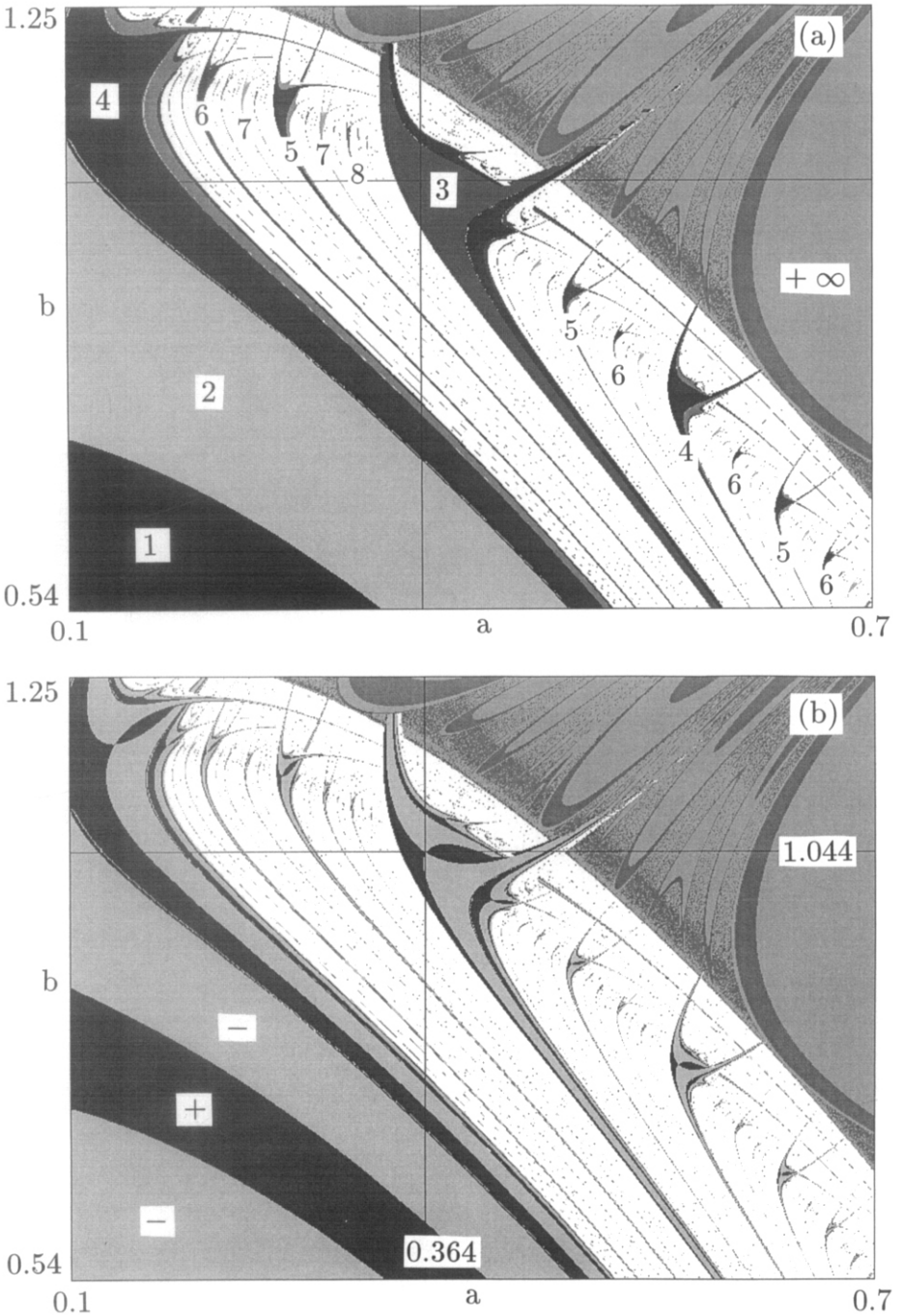

Fig. 3. Magnified view of the upper region in fig. 2, concentrating many shrimps along the direction defined by the head locus. (a) Isoperiodic domains, numbers indicating periods; (b) parity of multipliers, eq. (4.2). Shrimps are diffeomorphic copies of shrimps.

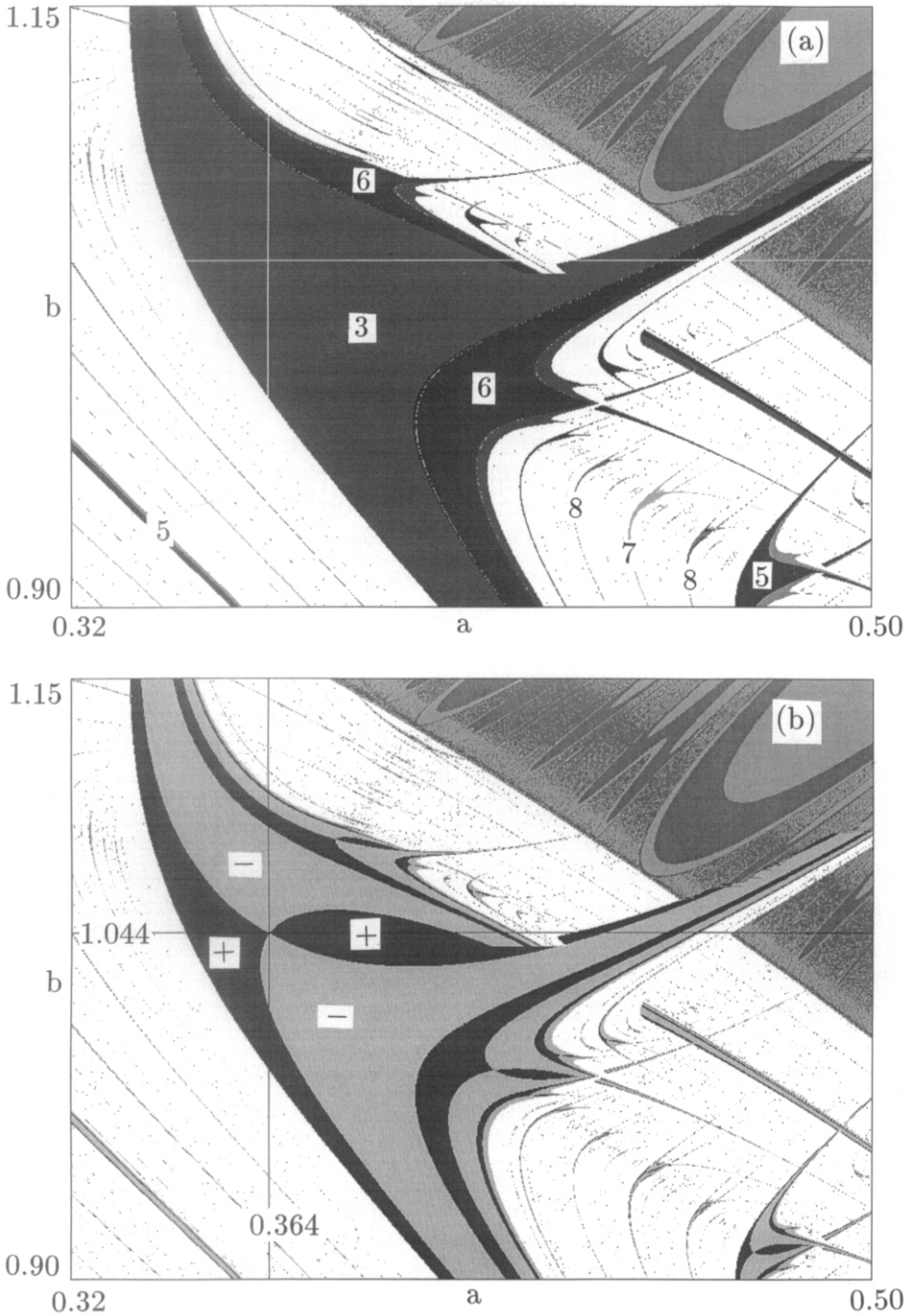

Fig. 4. Magnification of the period-3 shrimp shown in fig. 3, with the lines crossing at $a \simeq 0.364636$ and $b \simeq 1.044223$ indicating the location of the head. (a) Regions of stability, numbers indicating periods; (b) parity of multipliers, eq. (4.2). Heads are *unique* saddle points inside each cell, dividing them into *quadrants*.

symmetry and the relative skewness of their main isoperiodic cell. The figures also give a recipe to obtain the numerical values of the parameters corresponding to heads and tails: look in the space of variables for degeneracies involving the zeros of the derivative. Inside each cell, the head H is the *unique saddle point* (a, b) for which the multiplier contains a *double zero* of the derivative of the map (double superstability). In the dual space of variables, this point corresponds to very particular orbits going simultaneously through both critical points of the map. Tails are slightly more subtle to be found. They also correspond to a degeneracy, not however to orbits going simultaneously through more than one zero of the derivative as for the heads, but instead, to that point (a, b) for which there are two different fixed-points of $f_k(x, a, b)$ (lying in different Riemann surfaces), each one corresponding to individual orbits of $f(x, a, b)$ containing a different zero of the derivative of the map.

From these definitions one sees that neighborhoods around the two fundamental points of each cell will invariably show characteristics of a quite distinct nature. Isoperiodic attractors are *non-degenerate* robust and independent of the initial conditions for a ball B_h of parameters containing the head. This implies primarily the existence of a *unique* basin of attraction for *all* orbits characterized by a common periodicity. In contrast, for balls B_t containing the tail one necessarily finds *degenerate* isoperiodic attractors, implying sensitive dependence on the initial conditions. Thus, because more than one isoperiodic attractor coexist for parameter values inside the tail ball (multistability), the global basin of attraction corresponding to all possible orbits sharing a common period is in fact the *union* of more than one sub-basins, each of them the basin of a *different* (but isoperiodic) attractor. These sub-basins exist for *extended* parameter domains showing that now, in sharp contrast with the situation depicted in fig. 1, multivalued multipliers occur not as *isolated points* but rather over *extended domains*. This phenomenon (extended domains of multivalued multipliers) explains why in all figures tails are not numerically as well defined as heads: tails are quite sensitive to the initial conditions used to compute periodicities. As seen from the figures, in some small *overlap* regions there are also basins of stable attractors with *different* periods coexisting concomitantly with the intertwining of basins of the several isoperiodic attractors described above. Such small (but far from measure-zero) regions are those where one finds the largest possible number of different stable attractors living together in a cell.

As a simple example, we now show how to locate exactly the head of period-3 shrimps of eq. (4.1), the first non-trivial ones. We already know that fixed-points of $f_k(x, a, b)$ corresponding to heads involve orbits of $f(x, a, b)$ that must pass through degenerate zeros of the derivative, in the present case, through $+\sqrt{a}$ and $-\sqrt{a}$. Let us start by choosing to go from $+\sqrt{a}$ to $-\sqrt{a}$.

Period-3 means eventually converging to the following forever repeating sequence of numbers:

$$\cdots \to x_0 = \sqrt{a} \to x_1 = -\sqrt{a} \to x_2 \to x_3 \equiv x_0 = \sqrt{a} \to \cdots . \tag{4.7}$$

Substituting x_1 and x_0 in eq. (4.1) one sees that these two points in this order will belong to the sequence of eq. (4.7) if and only if $b = (1 + 2a)\sqrt{a}$. With this x_1 and b replaced in eq. (4.1) one obtains $x_2 = -(1 + 4a)\sqrt{a}$, conspicuously showing the algebraic closure of the set of numbers ruling the dynamics of orbits through critical points. When replacing x_2 and b in eq. (4.1) (thereby completing the third iterate $x_3 \equiv x_0$) one obtains the condition defining the possible values of a, namely

$$32a^4 + 24a^3 - 2a - 1 = 0 . \tag{4.8}$$

This equation may be solved exactly. Approximate roots are enough for the argument here: $a \simeq 0.364636$, -0.713268 and $-0.200684 \pm i0.28263$. Since a must be real and non-negative to produce real fixed-points, there is a 3-periodic head located at

$$(a_h^+, b_h^+) = (0.3646364723\ldots, 1.044223829\ldots) . \tag{4.9}$$

Reversing the order of the points in eq. (4.7) produces $b = -(1 + 2a)\sqrt{a}$ and the same polynomial for a as in eq. (4.8). Therefore, there is another period-3 shrimp symmetrically located at

$$(a_h^-, b_h^-) = (0.3646364723\ldots, -1.044223829\ldots) . \tag{4.10}$$

Since eq. (4.1) has only two critical points and there is no other possible permutation of them while circulating through a period-3 orbit, one concludes that these two are the only period-3 shrimps possible for the map of eq. (4.1). More than to simply obtain the locations of heads, this example was intended also as a plausibility argument to show that though quickly increasing as the period grows, the *number* of periodic cells with any period k is perfectly *countable* and depends solely (i) on the number of zeros of the derivative of the map and (ii) on the number of different possibilities of visiting all permutations of groups of such zeros through the equation defining the physics. The number of different possibilities grows obviously fast with k. Regarding the relative visible volume of isoperiodic domains, note that sizes are determined as roots of those polynomials with "explosive" degrees mentioned previously and which can be shown to oscillate faster and faster as the period

increases. Accordingly, sizes decrease with the period in the same proportion, i.e. very fast.

Let Δ be the number of minimum possible iterates needed to move from one zero of the derivative to the next, for example, to go from $\sqrt{a}$ to $-\sqrt{a}$. All shrimps having degenerate zeros appearing immediately following each other, i.e. having $\Delta = 1$, will live along either the "1^+-ray" $b = (1+2a)\sqrt{a} = +\sqrt{a + 4a^2 + 4a^3}$ (if. . . $\to \sqrt{a} \to -\sqrt{a} \to$. . .) or along the "$1^-$-ray" $b = -(1+2a)\sqrt{a} = -\sqrt{a + 4a^2 + 4a^3}$ (if. . . $\to -\sqrt{a} \to \sqrt{a} \to$ . . .). For example, both 5-shrimps with heads approximately at (0.3955724609987. . . , $\pm$1.1265325656333. . .), derived from the unique real and non-negative root a of a polynomial of degree 121. $\Delta = 2$ shrimps will exist along rays which contain, for example, points obtained by substituting each one of the two real roots of $64a^4 - 12a^2 - 6a + 1 = 0$ into the equations $b = \pm\sqrt{1 + 3a - 12a^3}$. They correspond to four 4-shrimps located roughly at (0.1341351918. . . , $\pm$1.171940. . .) and (0.553103312. . . , $\pm$0.792986. . .). By plotting several similar locations on a single graph one realizes that they all divide the "big fish" seen in fig. 2 into a more or less concentric infinite number of "onion-shells", well approximated by Tschirnhausen-like cubics of the generic type $\kappa b^2 = (r_1 - a)(a + r_2)^2$. The aforementioned "rays" run roughly perpendicular to these shells. In addition to containing the shrimps with heads defined by eqs. (4.9) and (4.10), the most prominent direction of shrimp-alignment is defined by the curve containing the "fat shrimps" (those larger and more readily discernible in the figures, defining almost visually the alignment locus). This curve contains two branches which cross each other at the very important 4-shrimp with head defining a center of symmetry at exactly $b = 0$ and $a = \sqrt{(3+\sqrt{17})/8} \simeq 0.9436038381\ldots$. This salient curve corresponds to the locus called α-direction in ref. [14]. The exceptional symmetry centered around this 4-shrimp may be seen in colors in fig. 7 of ref. [19], where it is shown for the 6-shrimp of the $+x_t^3$ cubic. Several diagrams derived from the analysis of the algebraic structure underlying the dynamics ruling the very regular distribution of shrimp clusters in parameter space will be presented elsewhere.

5. Anatomy of a few more complex shrimps

A recent paper [24] has shown that the $\tau = 1$ family of non-Markovian processes described by $x_{t+1} = a - x_{t-\tau}^2$ contains routes to chaos that are *degenerate* with the familiar doubling route $1 \to 2 \to 4 \to 8 \to \ldots$ known to be present in unimodal maps having 'quadratic extrema' such as $x_{t+1} = a - x_t^2$. The $\tau = 1$ process can be written as a two dimensional discrete map:

$$x_{t+1} = a - y_t^2 , \qquad y_{t+1} = x_t . \tag{5.1}$$

Fig. 5 shows "generalized bifurcation trees" comparing $(x, y) \mapsto (a - x^2, x)$ (a 2D embedding of the familiar period-doubling route) and the new degenerate route [24] as obtained from eq. (5.1). As seen from the figure, eq. (5.1) presents a *hiccup* route $1 \to 4 \to 8 \to \ldots$, i.e. a route in which subsequently to the region characterized by fixed points one finds a period quadrupling instead of the familiar period doubling. As it is not difficult to realize, this quadrupling comes from the delay introduced by the equation of motion $y_{t+1} = x_t$: although sequences of values generated by eq. (5.1) are numerically identical to those generated by the quadratic map, in this new map one has to wait a proper number of "clock units" for sequences of now *two* points to repeat. As already discussed in refs. [21,24], the delay-mechanism implied by the equation $y_{t+1} = x_t$ is rather common for a large class of processes and allows an extremely rich variety of possibilities for "composing" the dynamics.

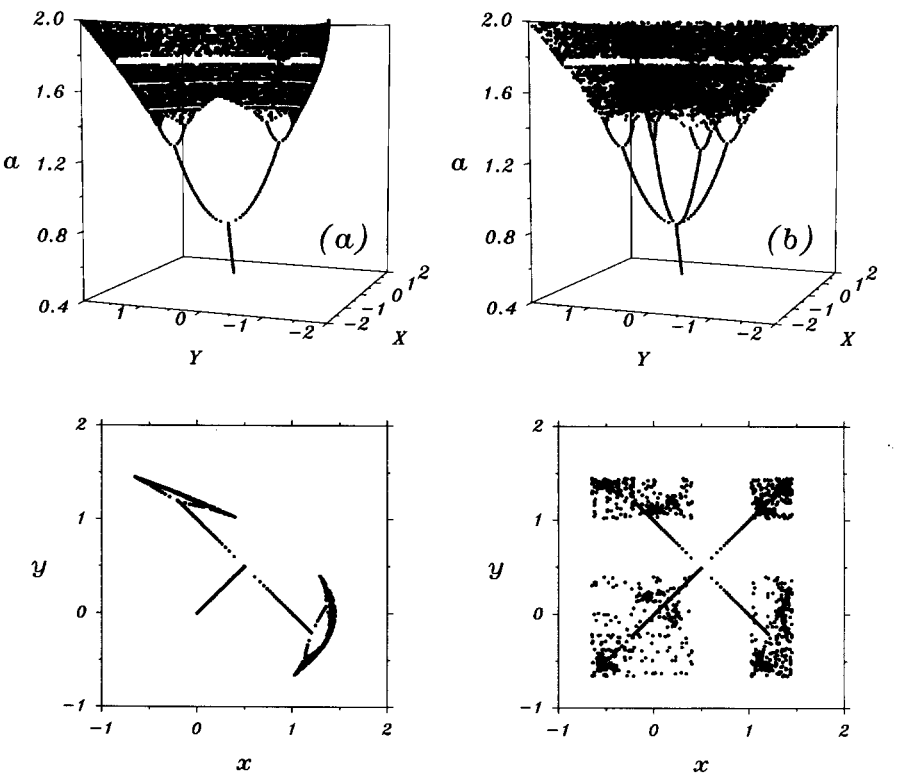

Fig. 5. The two degenerate routes to chaos: (a) for the 2D embedding of the quadratic map defined by $(x, y) \mapsto (a - x^2, x)$; and (b) for the map of eq. (5.1): $(x, y) \mapsto (a - y^2, x)$. This is one example of parametrically coupled oscillators.

Of particular interest for this paper is to consider the most general process leading to the *same* type of shrimp shapes and ordering found in the previous section for the cubic map (see ref. [19] for detailed color pictures of many high-period clusters of stability) and for the Hénon map [14]. By considering the dynamics of eq. (5.1) as done in ref. [24] one sees that this can be achieved coupling, i.e. *synchronizing* two quadratic maps in the following simple way:

$$x_{t+1} = a - b - y_t^2 , \tag{5.2a}$$

$$y_{t+1} = a + b - x_t^2 . \tag{5.2b}$$

This 2D map displays the same hiccup route $1 \to 4 \to 8 \to \ldots$ as eq. (5.1). Exploring memory effects of the "internal clock" of the system one may also realize how to further simplify, synchronize and build a corresponding one-dimensional (now *trimodal*) model presenting the same basic dynamics as both eqs. (5.1) and (5.2):

$$x_{t+1} = (a - b - x_t^2)^2 - (a + b) . \tag{5.3}$$

Exactly as previously found [24] for the map of eq. (5.1) and for the aforementioned 2D embedding of the quadratic map, eq. (5.3) presents the *same borders* in parameter space as eq. (5.2) but now, as expected due to the double composition, with adjacent cells following the familiar doubling route instead of the new hiccup route. All three maps, eqs. (5.1), (5.2) and (5.3) are particularly interesting highly degenerate situations for which it is possible to obtain a number of analytical results relatively easily. With the same conventions as before, fig. 6 presents the degenerate parameter space corresponding to *both* the one-dimensional dynamical systems of eq. (5.3) and the two-dimensional system of eq. (5.2). Contours in the parameter space for both models are exactly the same, the only difference being that when dealing with the two-dimensional map, similarly to what happens for the degenerate routes shown in fig. 5, instead of period k one has period $2k$ for all $k > 1$. Apart from this degeneracy, fig. 6 is also highly symmetric with the first two heads and the first tail occurring at very particular and convenient numerical values.

Yet another interesting example of a dynamical system is provided by the model

$$x_{t+1} = [(a - b)^2 - x_t^2]^2 - (a + b) , \tag{5.4}$$

closely related to that of eq. (5.3). This example is intended to show that when iterating nonlinear functions, not only nonlinearities in the *variables* are important, but that the structure of the parameter space will be also affected by

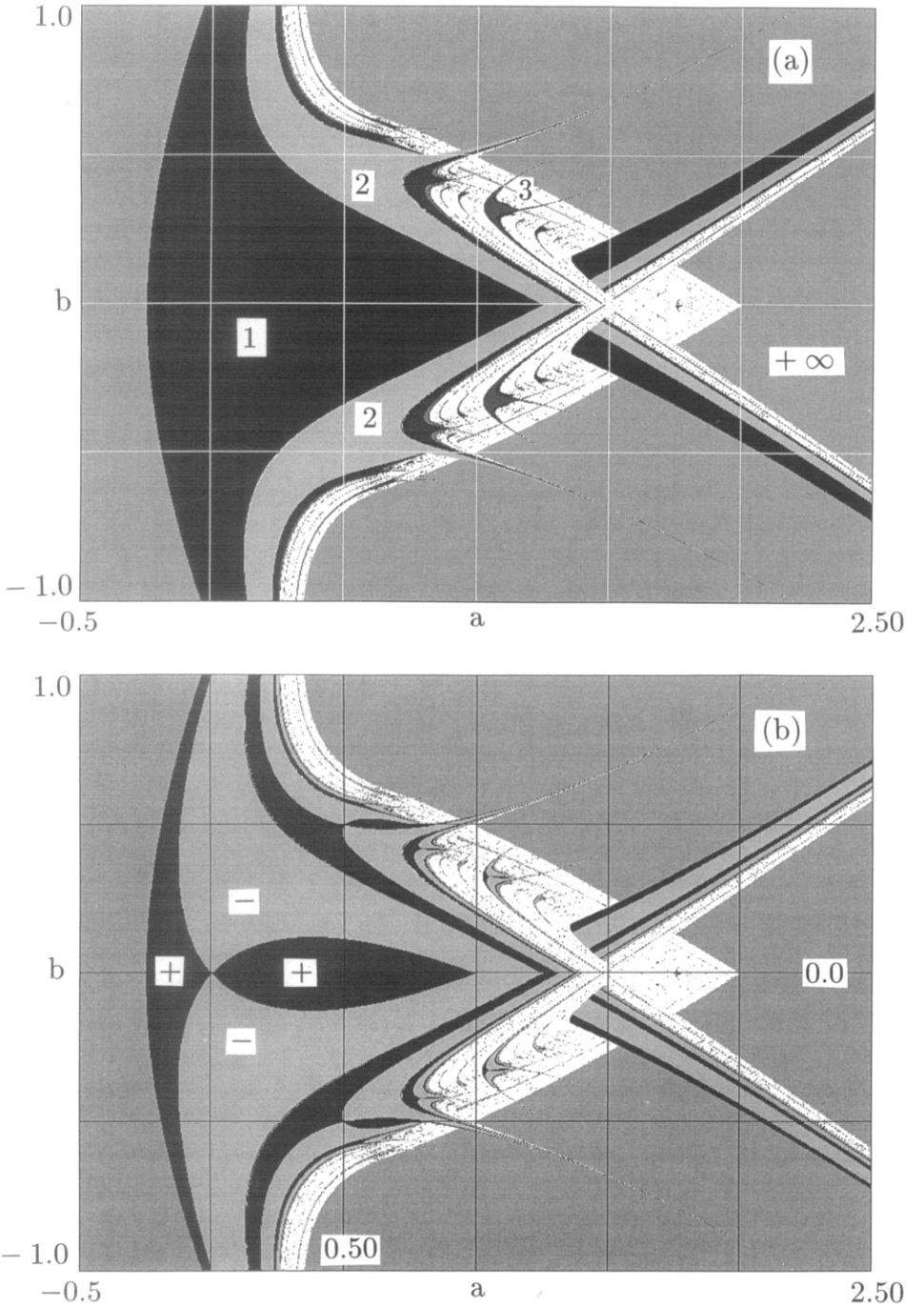

Fig. 6. Basic symmetric and degenerate stability structure corresponding simultaneously to the 2D map of eq. (5.2), the 1D map of eq. (5.3) and several others [24]. (a) Isoperiodic domains, numbers indicating periods for eq. (5.3); (b) parity of multipliers. Note the *self-inverse* nature of superstable loci.

all sorts of nonlinearities eventually present in the *parameters*. The reason for this can be recognized by considering the location of the zeros of the multipliers. The multiplier of eq. (5.3) involves products of $4x[x^2-(a-b)]$ while that of eq. (5.4) contains $4x[x^2-(a-b)^2]$. Apart from $x=0$, the multiplier of eq. (5.3) has zeros at

$$\sqrt{a-b}\,, \quad \text{and} \quad -\sqrt{a-b}\,. \tag{5.5}$$

The nontrivial zero derivatives of eq. (5.4), however, are located at

$$|a-b| \quad \text{and} \quad -|a-b|\,. \tag{5.6}$$

This means that in sharp contrast with eq. (5.5), eq. (5.6) will now have *real* critical points for $a-b<0$. One sees that while the map of eq. (5.3) might perhaps correspond to a kind of "fundamental" possibility of spreading zeros of the derivative in the parameter space, as shown by eq. (5.4) it is quite far from being a *unique* possibility. A further point worth noticing is that as the main period of the stability clusters increases, in addition to the central body which is relatively easy to detect numerically, it is possible to find for some high-dimensional systems several further structures of many different forms (e.g. cusp-like) along the prolongation of some "legs" and in other places [14a]. For example, such structures appear in specific locations along the legs which are seen to penetrate the region of parameters where most of the initial conditions lead to divergence. At these specific places the legs change their relatively smoothly varying original orientation, being abruptly deflected into a quite different direction. The location of these "measure zero" parameter regions corresponds to zeros of high-degree polynomials (obtained similarly as eq. (4.8)) and having relatively large a and/or b coordinates. Being zeros of very high degree polynomials, such regions are quite small and usually relatively hard to detect numerically. As the period increases, this behavior implies the possible existence of one or more places along the $m=0$ locus where there are discontinuities of derivatives. To locate such regions requires using accurately chosen initial conditions. In other words, such regions are relatively "transparent" to the majority of initial conditions.

6. The fundamental period-1 cell

The aim of this section is to describe with more detail the structure of the fundamental period-1 cell of stability and to define the location of the ten noble points of degeneracy in it. We will also argue that knowledge of the bifurcation

structure for the 1-shrimp might be eventually sufficient to characterize that of all higher-periodic k-shrimps.

Fig. 7 shows the period-1 cell of stability corresponding simultaneously to both dynamical systems defined by eqs. (5.2) and (5.3). This cell of stability is the same seen in fig. 6 but, to enhance the symmetry on the parameters, it is shown here rotated counterclockwise by 45 degrees, i.e. having $a - b$ replaced by a and $a + b$ replaced by b, respectively, in both equations. As the figure shows, this cell contains altogether ten noble points of degeneracy. The primary points H and T are the intersections of the dotted *self-inverse* parabolic curves which correspond to the locus of $m = 0$ values. As explained before, while H corresponds to a true intersection of the parabolas, T is just a pseudo-intersection since each $m = 0$ parabola is located at different x quotas (i.e. in different Riemann surfaces). Collinear with H and T one sees the points C and R, which together with points A, *above* the axis, and B, *below* the axis, form a "kite" at the end of the cell. A is located at $(a, b) \simeq (1.01905888, 1.16529086)$, while B appears symmetrically at $(1.16529086, 1.01905888)$. Fig. 7 also shows the location of four additional points of degeneracy. From the figure it is clear how to obtain them: looking for all the remaining possible combinations of pairs of intersections of the $m = -1, 0$ and $+1$ lines. These four points are not particularly relevant for our purposes and, accordingly, will not be further discussed here.

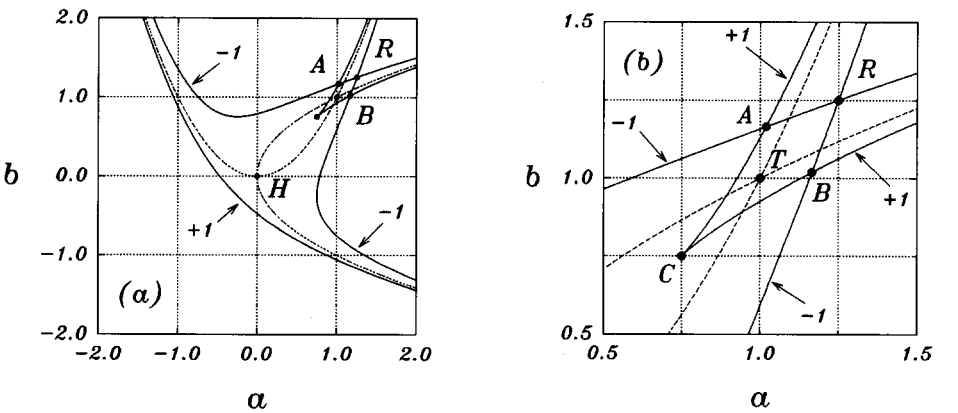

Fig. 7. Structure of the fundamental period-1 cell of stability, showing the location of the ten noble points of degeneracy. Numbers refer to the values of m. (a) Definition of the head H and the "collineation triangle" through the points H, A and B; (b) detail showing the *kite* formed by the points C, A, R and B. The tail is represented by the letter T. The points H, C, T and R lie all on the axis of symmetry. The two self-inverse parabolas intersecting at H and pseudo-intersecting at T are the locus of $m = 0$ (superstable) orbits.

By comparing figs. 6 and 1 with fig. 7 one sees that now, rather than having multivalued multipliers occurring at simple and isolated border points, multivaluedness clearly exists over extended parameter domains. In particular, multivaluedness (with corresponding intertwined basins of attraction) exists in the "complicated V" domain, i.e. at the borders and inside the two infinitely long legs obtained as upward prolongations of the curves C − A and B − R (first leg) and C − B and A − R (second leg). As seen in figs. 1 and 6, as parameters increase past the $m = -1$ borders there is either a period-4 (for eq. (5.2)) or period-2 (for eq. (5.3)) bifurcation. Therefore, inside the domain starting at the upper-right corner in fig. 7b and containing the letter R one finds a characteristic build-up of the multivaluedness, double that occurring before entering this domain. As clear from fig. 6, such legs are quite long, in fact infinitely long, but then for exceptionally narrow intervals of stability. The situation described for the period-1 cell recurs for all other cells, with corresponding noble points and singularity loci being connected through families of affine-like transformations. Preliminary results obtained by considering the interrelation of triplets (x, a, b) and the equations of motion defining the singularity loci present in the unit cell shown in fig. 7 indicate that for any domain containing parameters (a_0, b_0) for which degenerate orbits x_t occur with multiplicity μ, one will necessarily have singularities behaving as powers of $1/\mu$ in parameter space. This result is useful to obtain analytical relations between triplets (x, a, b) defining singularity loci in parameter space [25]. In particular, it allows one to obtain for cubic maps two basic shrimp shapes: one involving shrimps with main cells of parabolic curvature, arising from parameter singularities behaving like powers of 1/2, and another one involving shrimps with cusp-like main cells, arising from singularities behaving like powers of 1/3. This latter type of singularity is the same one responsible for the so-called [1–9] "Arnold tongues" while the former is responsible for parabolic-shaped cells similar to those discussed here and in ref. [14]. Detailed color pictures for these two shapes as obtained for cubic maps are given in ref. [19].

Since *any two triangles are related by a unique affine collineation* [26], we may conveniently elect, for example, the points H, A and B to explicitly obtain affine transformations connecting cells of different periodicity (and different shrimps). For this choice of triangles the affine transformation connecting shrimps having main periodicities $1 \to 3 \to 9 \to 3^j \ldots$ with $j = 0, 1, 2, \ldots$ (corresponding to the *uppermost* nested sequence of windows above the line $b = a$) is well approximated by

$$a' = 0.07837a + 0.02807b + 0.72543\,, \tag{6.1a}$$

$$b' = 0.03271a + 0.05661b + 1.37799\,. \tag{6.1b}$$

If (a, b) is in the 1-shrimp, then (a', b') defined by eq. (6.1) will be the corresponding point located in the 3-shrimp (that indicated by the number 3 in fig. 6a), with subsequent j compositions being (approximately) in shrimps of main periodicity 3^j. Eq. (6.1) maps *all* isoperiodic domains composing the shrimp simultaneously, not just the period k cell. To our knowledge, eq. (6.1) is the first one ever given showing how to connect a doubly-infinite number of domains of stability in the space of parameters which correspond to completely different physical behaviors in the space of variables. If proved valid for the full extent of the unit cell, transformations like that defined by eq. (6.1) would show that period-3 as well as all other subsequent 3^j shrimp windows, rather than corresponding to something new, are just affine repetitions of the phenomena contained in the fundamental period-1 shrimp with main cell described in fig. 7. This quite interesting consequence of the algebraic analysis does not seem to have been anticipated before. Our numerical evidence shows such scenario to be a quite good approximation of the situation found. Knowledge of a possible "first cell/shrimp reduction" is of interest because it would allow greatly simplifying the study of stability domains by breaking it into two broad problems: (i) to understand the detailed anatomy of the period-1 cell/shrimp and (ii) to study which groups of transformations spread them in the whole space of parameters. Note that since stability domains for the dynamical systems defined by eqs. (5.2) and (5.3) are degenerate, eq. (6.1) is simultaneously valid for different physical models. In fact, we believe the results presented here to provide heuristic evidence that the period-1 shrimp dissected in figs. 6 and 7 is a kind of "canonical" one for an extremely large family of physical models (all those characterized by singularity loci behaving as powers of 1/2), and which would all display just sequences of *copies* of it. Thus, once understood how bifurcations occur for the fundamental shrimp, the problem of characterizing domains of stability for physical models of interest would amount to studying the proper *group* of transformations implied by their equations of motion.

Transformations similar to that of eq. (6.1) allow one to easily "fish little shrimps" of any periodicity living in domains (a', b') (along with all microstructures belonging to them) by "transporting" them onto the fundamental structure in the domain (a, b) seen in figs. 6 and 7, a parameter range where they can be more comfortably dissected. For this purpose, instead of the HAB isosceles triangle used to obtain eq. (6.1), a more convenient choice from the point of view of locating vertices of triangles numerically is to use the "H^3" triangle formed by the heads of the three first larger cells of the shrimp. As easy to recognize from fig. 7 however, up-side down isosceles triangles (with basis simultaneously tangent, say, to both $m = -1$ borders of the main cell and with opposite vertex located somewhere above the tail) are expected to

produce much better overall fits although parameters for them might be somewhat harder to obtain numerically for arbitrary k.

7. Conclusions

The main purpose of this paper was to delimit the full extent of certain shrimp-like clusters of stability and to explain the great regularity with which they are seen to appear in the parameter space of representative dynamical systems which arise when modeling nonlinear physical phenomena with discrete-time models. Using the parity of multipliers we argued that the $k \times 2^n$ isoperiodic clusters heuristically described in refs. [14,19,21] for the Hénon, cubic and other maps, are generated by a countable infinite sequence of repetitions of a basic elementary cluster, this elementary cluster being itself composed of affine-like repetitions of the elementary "unit cell" reproduced in fig. 7. Every isoperiodic cell for the dynamical systems discussed here (which are representative of a large class of models) contains two primary noble points of degeneracy with a line segment through them being an axis of approximate symmetry of the cell. The orientation of every $k \times 2^n$ shrimp in parameter space is defined essentially by the orientation of the axis of their main cell and its skewness. The peculiar directions along which shrimps were previously found [14] to align are formed as the locus of the main head of several $k \times 2^n$ shrimps. These simple directions are generic and arise as intrinsic consequences of the peculiar algebraic structures resulting from the occurrence of certain degenerate fixed-points of $f_k(x, a, b)$. The corresponding orbits obtained by considering iterates of $f(x, a, b)$ will contain in this case one or more critical points of the equations of motion ruling the dynamics.

We also reported two dynamical systems (eqs. (5.2) and (5.3)) that in spite of having different dimensions and displaying different routes to chaos, display exactly the same arrangement of borders of stability in parameter space. We emphasized the role of nonlinearities present in parameters, not only in variables. While it might be tempting to conclude some of the systems discussed here to represent perhaps a kind of "universality" intrinsic to bimodal maps, from the discussion and figures of ref. [24] one sees that there are several other possible compositions presenting "generalized" shrimps having shapes rather different from that discussed at length in this paper. The precise delimitation and classification of all possible fundamental shapes for domains of stability in the parameter space would be certainly of considerable interest and, as preliminary results indicate, is anticipated to depend strongly on the multiplicity μ of fixed points of $f_k(x, a, b)$ along loci of degeneracy. Section 6 presented a number of consequences derived from the structure-

parallel-to-structure affine symmetry present in the space of parameters and argued that knowledge of the bifurcation patterns for the 1-shrimp should suffice to understand that of all other shrimps. We would also like to add to have empirically observed that for many (mainly polynomial) systems investigated so far there is frequently a quite regular periodicity pattern according to which shrimps appear to organize themselves along the head locus: the largest isoperiodic shrimps with period not smaller than k appearing along the locus simultaneously on both sides of a shrimp of main period k and having approximately the same visible area, seem to always have period $k+j$, j an integer, apparently always either 1 or 2, depending on the equations of motion.

A quite interesting result is the symmetry and high degeneracy of the parameter space of eqs. (5.2) and (5.3). For these equations it is possible to derive analytically a number of features and, in particular, to hope to be able to eventually find an analytical expression for the head locus defining the principal shrimp alignment. Preliminary results indicate all these regular features to arise as projections along the real line of a regular finite lattice with vertices formed by certain commensurability properties of the parts composing the aforementioned generalized numbers and which are implicitly contained in the equations of motion. For systems with one variable and two parameters (a, b) as here, adjusting a is equivalent to choosing initial conditions that define the algebraic structure of the set of roots that may be reduced to the form $u_j + v_j\sqrt{a}$. Then, by simultaneously adjusting a and b, one may bring the system to privileged (but rather abundant) locations in the parameter space such that the dynamics observed in the space of variables will periodically cycle through some of all possible vertices (those not defined by complex numbers) of a kind of polygon where the full dynamics lives. The location of such vertices depends on u_j^2, v_j^2, a and $-a$, quantities which also define the singularity loci and the noble points of degeneracy. This whole picture arises because for particular but infinite in number combinations of parameters, "resonances", the dynamics succeeds in eluding and evading most of the many prisons of being under square and cubic root signs similarly as the following few of an infinite series of possible identities show

$$2 = \sqrt[3]{7+\sqrt{50}} + \sqrt[3]{7-\sqrt{50}} = \sqrt[3]{\sqrt{108}+10} - \sqrt[3]{\sqrt{108}-10}$$
$$= \sqrt{\sqrt[3]{26+15\sqrt{3}} + \sqrt[3]{26-15\sqrt{3}}} = \sqrt{4}\,.$$

It would be of interest to investigate the $+x_t^3$ normal form of the cubic map [19]. As shown in ref. [19], $+x_t^3$ cubics present shrimp shapes fundamentally different from that typical for the $-x_t^3$ cubic discussed here. Stability structures for $+x_t^3$ cubics involve mother cells similar to the well-known Arnold tongues

[15–17] obtained for circle maps when congruences involved in the definitions of these maps are removed. Such congruences appear to be non-essential since it is possible to produce full cascades of Arnold tongues using polynomial dynamical systems without congruences, for example, with the system [24] $(x, y) \mapsto (a - py^2 - qx^2, x)$. Circle maps are very important models, frequently used to describe quasiperiodicity in natural phenomena.

We conclude by observing that in 1799 Gauss proved the so-called "fundamental theorem of algebra" (ref. [26], page 144), asserting the *existence* of roots for polynomials of any arbitrary degree, even when expressions for the roots are not obtainable. Unfortunately, as of this date there is no prescription to obtain the *number* of real roots for a polynomial of arbitrary degree, not even for particular cases when some not too restrictive relations are known to hold among arbitrary coefficients. Knowledge of such information is equivalent to classifying all possible bifurcations (singularity loci) for polynomial models, an extremely interesting and needed result for practical applications. For example, to delimit the extent of stability regions of periodic motions in physical models.

Note

A recent paper by J. Milnor (Exp. Math. 1 (1992) 5), among several other things, discusses the dynamics of iterated cubic maps and the *connectedness locus* for eq. (5.3). This locus is different from the superstable locus and from the locus discussed in the present paper. I thank Prof. Milnor for giving me this reference and for helpful discussions and suggestions.

Acknowledgements

The friendly criticism and helpful suggestions of Hans J. Herrmann, Jülich, and Helena E. Nusse, Groningen, are gratefully acknowledged. I am also grateful to Profs. C. Grebogi and J.A. Yorke for their kind interest in my work.

References

[1] H.-O. Peitgen, H. Jürgens and D. Saupe, Chaos and Fractals, New Frontiers of Science (Springer, New York, 1992).

[2] A.J. Lichtenberg and M.A. Lieberman, Regular and Chaotic Dynamics, 2nd ed. (Springer, New York, 1992).
[3] J. Guckenheimer and P. Homes, Nonlinear Oscillations, Dynamical Systems, and Bifurcations of Vector Fields, 3rd printing (Springer, New York, 1990).
[4] P. Manneville, Dissipative Structures and Weak Turbulence (Academic Press, Boston, 1990).
[5] P. Cvitanovic, Universality in Chaos (Adam Hilger, Bristol, 1989).
[6] H. Bao-Lin, Chaos II (World Scientific, Singapore, 1989).
[7] R.L. Devaney, An Introduction to Chaotic Dynamical Systems, 2nd ed. (Benjamin Cummings, Menlo Park, 1988).
[8] C. Mira, Chaotic Dynamics (World Scientific, Singapore, 1987).
[9] P. Collet and J.-P. Eckmann, Iterated Maps on the Interval as Dynamical Systems (Birkhäuser, Basel, 1980).
[10] J.E. Marsden and M. McCracken, The Hopf Bifurcation and its Applications (Springer, New York, 1976).
[11] M. Feigenbaum, J. Stat. Phys. 19 (1978) 25; 21 (1979) 669.
[12] S.J. Chang, M. Wortis and J. Wright, Phys. Rev. A 24 (1981) 2669.
[13] H. El Hamouly and C. Mira, C.R. Acad. Sc. (Paris), Série I 293 (1981) 525; 294 (1982) 387.
[14] (a) J.A.C. Gallas, Int. J Mod. Phys. C 3 (1992) 1295;
(b) Phys. Rev. Lett. 70 (1993) 2714.
[15] L. Glass and R. Perez, Phys. Rev. Lett. 48 (1982) 1772;
L. Glass, M. Guevara, A. Schrier and R. Perez, Physica D 7 (1983) 89;
L. Glass, M.R. Guevara, J. Bélair and A. Schrier, Phys. Rev. A 29 (1984) 1348;
J. Bélair and L. Glass, Physica D 16 (1985) 143;
L. Glass, Chaos 1 (1991) 13.
[16] M. Schell, S. Fraser and R. Kapral, Phys. Rev. A 28 (1983) 373;
J. Ringland and M. Schell, Europhys. Lett. 12 (1990) 595.
[17] R.S. MacKay and C. Tresser, Physica D 19 (1986) 206; 27 (1987) 412.
[18] S. Fraser and R. Kapral, Phys. Rev. A 25 (1982) 3223.
[19] F. Cabral, A. Lago and J.A.C. Gallas, Int. J. Mod. Phys. C 4 (1993) 553.
[20] J. Milnor and W. Thurston, Lecture Notes in Mathematics, vol. 1342 (Springer, Berlin, 1988).
[21] J.A.C. Gallas, Physica A 195 (1993) 417; 198 (1993) 339, errata.
[22] P. Fatou, Bull. Soc. Math. Fr. 47 (1919) 161; 48 (1920) 33.
[23] G. Julia, J. Math. Pures Appl. 4 (1918) 47.
[24] J.A.C. Gallas, Degenerate routes to chaos, preprint HLRZ 31/93; Phys. Rev. E, in print.
[25] J.A.C. Gallas, manuscript in preparation.
[26] H.S.M. Coxeter, Introduction to Geometry, 2nd printing (John Wiley, New York, 1962) p. 203.